Expanded View Figures

Figure EV1. Specificity of anti-Nrg3 and anti-ErbB4 antibodies, Nrg3/ErbB4 co-clustering on PV-negative neurons, and ErbB4 interneuron numbers in the hippocampus of Nrg3 mutant mice.

A, B Hippocampus sections from wildtype (A, B) and *Nrg3*$^{-/-}$ mice (A′, B′), age P35, were immunostained for Nrg3 (A, A′) and ErbB4 (B, B′). Nrg3 is widely distributed throughout the neuropil with higher levels being associated with ErbB4^{+} interneurons (A). Nrg3 immunostaining is abolished in Nrg3 mutant tissue (A′), ErbB4 levels are unchanged (B, B′).

C Western blot analysis of lysates from cortical tissue (brain) and cultured cortical neurons (culture). The anti-Nrg3 antibody detects a main band of about 95 kD (arrow) in lysates from wildtype (+/+) but not from Nrg3 mutant mice (−/−).

D Hippocampus sections from wildtype (D) and heart-rescued ErbB4 mutant mice (D′), 2 months of age, were immunostained for ErbB4. ErbB4 immunostaining is detected in wildtype (D) but not ErbB4 mutant hippocampus (D′).

E Western blot analysis of lysates from cortical tissue. The anti-ErbB4 antibody detects a main band of 180 kD (black arrow) and a minor band of about 70 kD (gray arrow) in lysates from wildtype (+/+) but not from ErbB4 mutant mice (−/−).

F Hippocampus section was immunostained against pro-CCK, ErbB4, and Nrg3; shown is the stratum pyramidale of CA1. CCK^{+} interneurons express variable amounts of ErbB4 as indicated by white (high expression), gray (middle), and open arrowheads (no detectable ErbB4). Association of Nrg3 with soma or dendrites of CCK^{+} interneurons is not detectable.

G Section of the prefrontal cortex was immunostained against Nrg3, ErbB4, and parvalbumin (Parv). Nrg3 is co-localized with ErbB4 on soma and dendrites of PV-positive (filled arrow and arrowheads) and PV-negative neurons (open arrow and arrowheads).

H Densities of ErbB4^{+} interneurons in different layers of the hippocampal CA1 region are identical in adult wildtype and Nrg3 mutant mice at postnatal days 90–120; so, stratum oriens; sp, stratum pyramidale; sr, stratum radiatum; slm, stratum lacunosum-moleculare. Data represent mean ± SD of six biological replicates for each genotype. Two-way ANOVA with Bonferroni's multiple comparisons test was performed to assess statistical significance (ns = not significant). Scale bars: 500 μm (D′), 40 μm (F″), 50 μm (G‴).

Source data are available online for this figure.

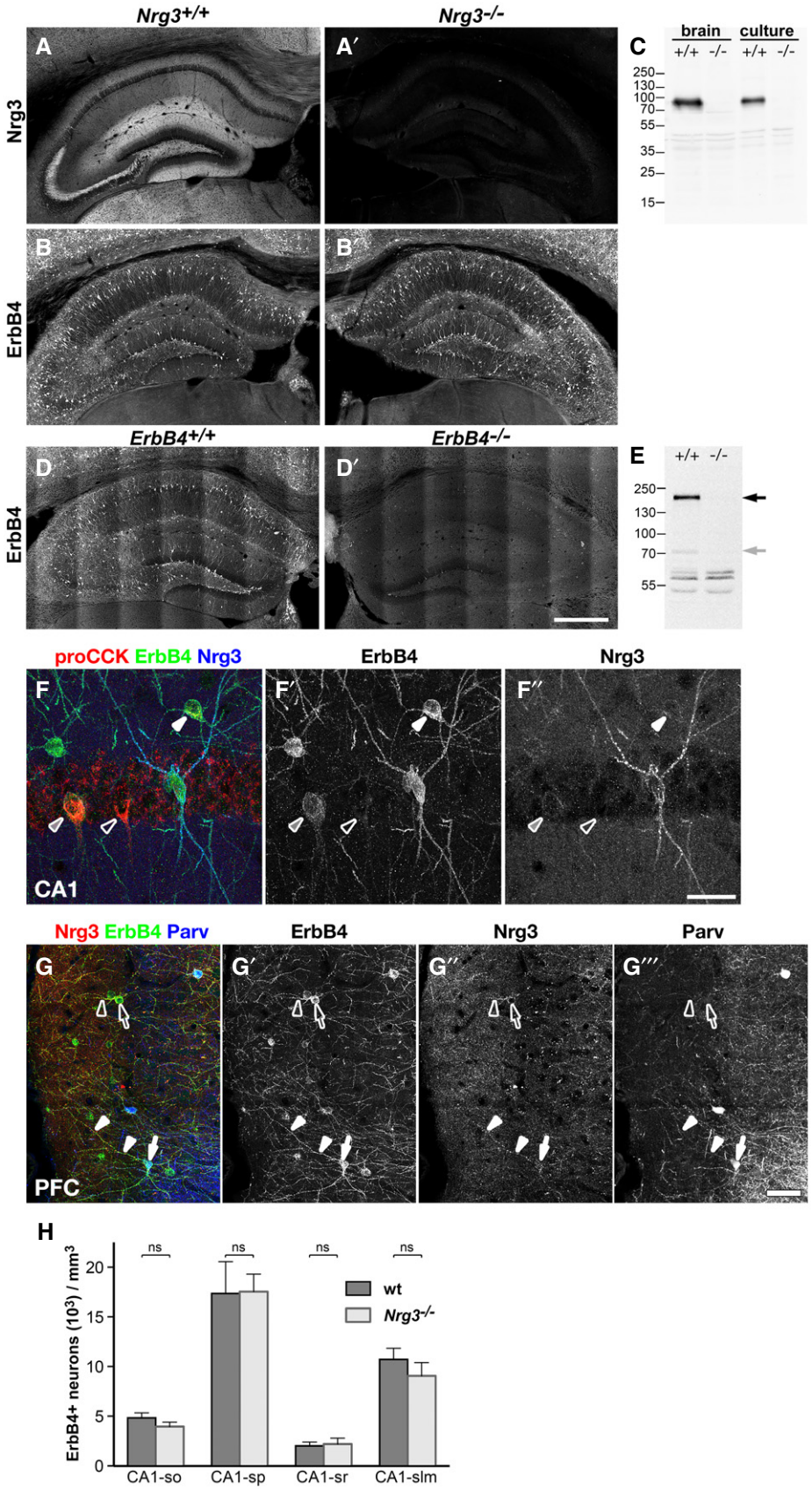
Nrg3+/+
Nrg3-/-
A
A′
Nrg3
B
B′
ErbB4
C
brain
culture
+/+ -/-
+/+ -/-
250
130
100
70
55
35
25
15
ErbB4+/+
ErbB4-/-
D
D′
ErbB4
E
+/+ -/-
250
130
100
70
55
proCCK ErbB4 Nrg3
ErbB4
Nrg3
F
F′
F″
CA1
Nrg3 ErbB4 Parv
ErbB4
Nrg3
Parv
G
G′
G″
G‴
PFC
H
ns
ns
ns
ns
wt
Nrg3-/-
ErbB4+ neurons (10³) / mm³
20
15
10
5
0
CA1-so
CA1-sp
CA1-sr
CA1-slm

Figure EV1.

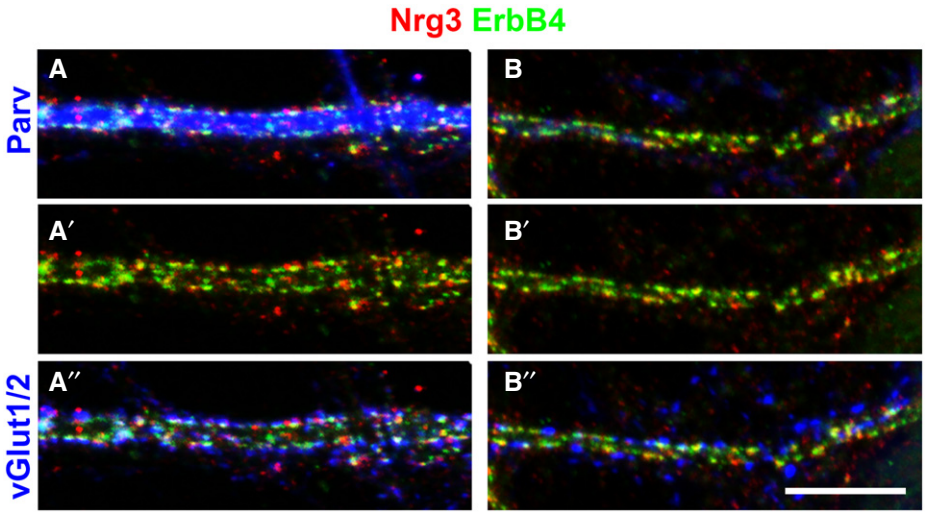

Figure EV2. Nrg3/ErbB4 co-clustering in cultured PV-positive and PV-negative interneurons.

A, B Neurons, cultured for 23 days, were co-immunostained with antibodies against Nrg3, ErbB4, parvalbumin (Parv), and vGlut1/2. Nrg3 and ErbB4 co-clustered on the dendrites of PV-positive (A) and PV-negative neurons (B). Note that (A–A″) and (B–B″) display false colors of the same images. Scale bar: 10 μm (B″).

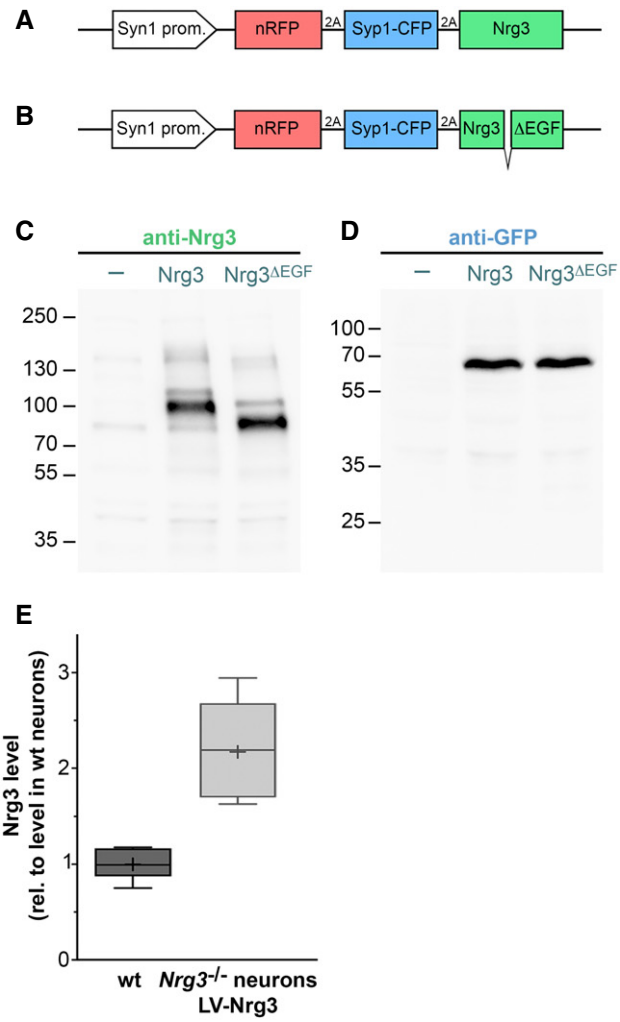

Figure EV3. Lentiviral expression of Nrg3 and Nrg3ΔEGF.

A, B Schematic display of the expression cassettes. The *synapsin I* (Syn1) promoter is used for neuronal expression. Coding sequences for red fluorescence protein with a nuclear localization sequence (nRFP) and a fusion protein of synaptophysin and the cyan fluorescent protein (SypCFP) are followed by coding sequences for Nrg3 (A) or Nrg3ΔEGF (B). nRFP, SypCFP, and Nrg3/Nrg3ΔEGF coding sequences are separated by 2A sequences.

C, D Comparison of Nrg3 (C) and SypCFP (D) expression levels in $Nrg3^{-/-}$ neurons that were transduced with the Nrg3/SypCFP (middle lanes) and Nrg3ΔEGF/SypCFP lentiviruses (right lanes) at high titer, respectively, by Western blot analysis using antibodies against Nrg3 (C) and GFP (D). The lanes indicated by (–) show lysates from non-transduced neurons as negative control. Both lentiviruses express similar protein levels of Nrg3/Nrg3ΔEGF and SypCFP. Note that the main Nrg3 band in lysates from neurons transduced with the Nrg3ΔEGF/SypCFP lentivirus is smaller due to the deletion.

E Immunocytochemical comparison of endogenous and lentivirally expressed Nrg3 levels in vGlut1/2+ excitatory synapses on ErbB4+ neurons in cultures of wildtype (wt, left) or $Nrg3^{-/-}$ neurons transduced with the SypCFP/Nrg3 lentivirus (right). Fluorescence levels were normalized to the mean fluorescence level in wildtype neuron cultures. The Nrg3 lentivirus produced 2.17 ± 0.14-fold higher Nrg3 levels than wt neurons, and n = 13 and 11 neurons were analyzed in cultures from wildtype and Nrg3 mutants, respectively. Data are presented as box plots with Tukey's whiskers and outliers. Plus symbols denote the mean.

F Hippocampal $Nrg3^{-/-}$ neurons after transduction with lentivirus expressing SypCFP/Nrg3 were analyzed by immunocytochemistry using antibodies against CFP, ErbB4, vGlut1/2, and GluA. Panels show the same image and display SypCFP/ErbB4, SypCFP/vGlut1/2, and SypCFP/GluA signals, respectively. The images were assigned false colors for better visualization of the signals. SypCFP, ErbB4, vGlut1/2, and GluA co-localize in excitatory synapses. Scale bar: 5 μm.

Source data are available online for this figure.

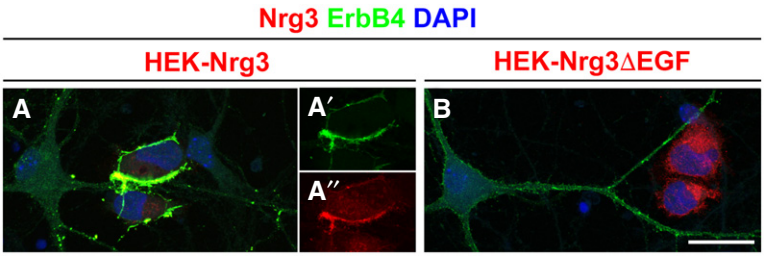

Figure EV4. Interaction of Nrg3- and Nrg3ΔEGF-expressing HEK293 cells with ErbB4$^+$ neurons.

A, B Neurons from Nrg3 mutant mice were co-cultured with (A) Nrg3- and (B) Nrg3ΔEGF-expressing HEK293 cells and immunostained for Nrg3/Nrg3ΔEGF (red) and ErbB4 (green). DAPI was used to counterstain nuclei (blue). Nrg3 and ErbB4 are highly enriched in contact areas between Nrg3-expressing HEK cells and ErbB4$^+$ interneurons (A); (A′ and A″) show lower exposures of the immunofluorescence signals of ErbB4 and Nrg3. Note that Nrg3ΔEGF and ErbB4 remained evenly distributed when an ErbB4$^+$ interneuron was contacted by an Nrg3ΔEGF-expressing HEK cell (B). Scale bar: 25 μm

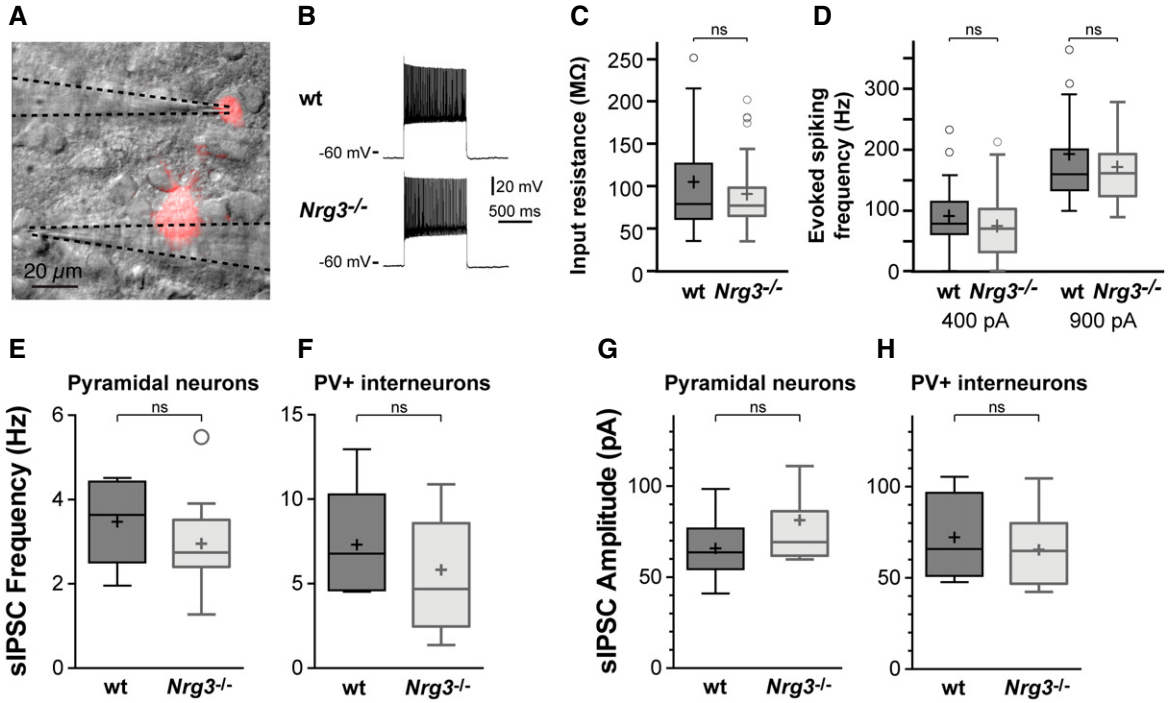

Figure EV5. Electrophysiological properties of PV interneurons in the hippocampal CA1 region of wildtype and Nrg3 mutant mice.

A Overlay of an infrared DIC image of the stratum pyramidale of the hippocampal CA1 with tdTomato fluorescence in a slice from a *Parv*$^{Cre/+}$;*Ai14*$^{flox/+}$ mouse. Dotted lines highlight the stimulation and recording electrodes.

B Example traces of the firing pattern of wildtype and *Nrg3*$^{-/-}$ PV interneurons. A current of 900 pA was injected for both patterns.

C Input resistance of PV interneurons in slices from wildtype and *Nrg3*$^{-/-}$ mice. Data from n = 59 (wt) and n = 55 (*Nrg3*$^{-/-}$) neurons from 20 wt and 30 mutant mice are displayed. Mann–Whitney U-test (unpaired, two-tailed) was performed to assess statistical significance (ns, not significant).

D Evoked firing frequency in PV interneurons from wildtype and *Nrg3*$^{-/-}$ mice after current injection of 400 pA (left) and 900 pA (right). Data from n = 59 (400 pA, wt), n = 55 (400 pA, *Nrg3*$^{-/-}$), n = 17 (900 pA, wt), and n = 41 (900 pA, *Nrg3*$^{-/-}$) neurons are displayed. Mann–Whitney U-test (unpaired, two-tailed) was performed to assess statistical significance (ns, not significant). No differences were detected in input resistance and evoked firing frequency between wildtype and *Nrg3*$^{-/-}$ mice.

E–H sIPSC recordings of pyramidal (E, G) and PV neurons (F, H) in acute slices. sIPSC frequencies (E, F) and amplitudes (G, H) are shown. Data from n = 6 wildtype and n = 11 *Nrg3*$^{-/-}$ pyramidal neurons and from n = 4 wildtype and n = 7 *Nrg3*$^{-/-}$ PV interneurons were analyzed using an unpaired two-tailed t-test, and no significant (ns) differences were detected.

Data information: Data in (C–H) are presented as box plots with Tukey's whiskers and outliers. Plus symbols denote the mean.